Computer Simulation Study on Comparing Lesion Effects of Radio Frequency Ablation for Treating Atrial Fibrillation by Multichannel Bipolar or Unipolar

Shengjie Yan [1], Xiaomei Wu [1,2,3+] and Weiqi Wang [1]

[1] Electronic Engineering Department, Fudan University, China

[2] Shanghai Engineering Research Center of Assistive Devices, Shanghai, China

[3] Key Laboratory of Medical Imaging Computing and Computer Assisted Intervention (MICCAI) of Shanghai, Fudan University, China

Abstract. Purpose: In pulmonary veins (PVs) isolation (PVI) and left atrial (LA) roof linear ablation, radiofrequency (RF) energy is often used to create a continuous lesion or discrete lesions for blocking the accessory conduction pathways. By using transient finite element analysis, this study compared the effectiveness of multichannel bipolar ablation mode (Multi-BiM) with unipolar ablation mode (UiM) in creating a continuous lesion and lesion size in a 5-mm-thick atrial wall. Methods: Computer models of unipolar and multipolar catheter were developed to study the length of continuous lesion and the size of discrete lesion in atrial walls created through Multi-BiM and UiM. Three peak value voltage—20 V 25 V and 30 V—were considered in Multi-BiM or UiM ablation (hereafter, Multi-BiM-20V, Multi-BiM-25V, Multi-BiM-30V and UiM-30V, respectively). Results: UiM-30V failed to create continuous and transmural lesion. Multi-BiM-20V created three discrete lesions. Multi-BiM-25V generated the continuous but not transmural lesion. Multi-BiM-30V not only created transmural lesions in 5-mm-thick atrial walls but also created continuous lesion with a maximum depth and width of 6.70 mm and 23.50 mm. An additional discrete lesion or short continuous lesion was yielded through multichannel bipolar ablation method with 30V ablation voltage. Conclusion: Compared with unipolar ablation, multichannel bipolar ablation can more easily create transmural lesions, continuous lesions and larger discrete lesion size in atrial tissue for completing circumferential PVI and LA linear ablation.

Keywords: Multichannel bipolar ablation, Radio frequency ablation, Continuous lesion, Transmural lesion, Computer model of finite element method.

1. Introduction

Atrial fibrillation (AF) is the most common cardiac arrhythmia in the general population. AF morbidity continuously increases with age. The common symptoms of AF include unpleasant and irregular heartbeats, impaired hemodynamic response caused by loss of atrioventricular synchrony, and vulnerability to thromboembolic complications [1]. Thus, a successful AF treatment has three positive consequences: it restores the sinus rhythm, normalizes cardiac hemodynamics, and alleviates the vulnerability to thromboembolism. In the past, common therapies for AF were antiarrhythmic drugs or the surgical maze procedure. However, both these approaches may entail high recurrence and severe injury during the open chest surgery. Circumferential pulmonary vein isolation and linear ablation in the left atrial roof have been demonstrated to be highly effective and reliable interventions against drug-resistant refractory AF [2], [3]. Conventionally, PVI and LA ablation are performed through point-to-point ablation using unipolar RF energy guided by an electromagnetic navigation system (Carto[TM], Biosense Webster, or Ensite[TM], St. Jude Medical) for reducing radiation exposure. This RF ablation technique delivers a sinusoidal voltage from the

---

[+] Corresponding author. Tel.: + 8602165642753;
E-mail address: xiaomeiwu@fudan.edu.cn

active electrode to the dispersive electrode and creates a discrete lesion slightly larger than the size of the active electrode tip [4]. In conventional unipolar ablation, continuous and linear lesions can be created by performing a series of discrete point ablation procedures, which requires a skilled operator; consequently, these procedures are often time intensive. Moreover, AF may recur because of incomplete linear lesion formation (i.e., presence of 'gaps'), resulting in partially recovered accessory conduction pathways.

Recently, the multichannel bipolar RF ablation technology has been clinically investigated for treating AF and the relevant finding is that the bipolar ablation for AF was substantially shorter of procedure time and a greater guarantee of transmural lesions compared with the unipolar ablation [5-7]. Therefore, developing multichannel RF ablation procedures that facilitate the easy creation of continuous lesions in PVs or LA is essential for treat AF. In this paper, by using transient finite element analysis, we established computer models to compare the effectiveness of multichannel bipolar ablation with unipolar ablation in creating continuous lesion and lesion size. A review of relevant literature revealed that no finite element model has yet been developed to compare the effectiveness of the multichannel bipolar ablation and unipolar ablation in creating continuous lesion and lesion size.

2. Method

2.1. Multichannel Bipolar Ablation Method

In the conventional unipolar ablation, the RF voltage delivers from the single active electrode to the dispersive electrode, leading to the unipolar current flow between active and dispersive electrodes, as illustrated in Fig. 1A. The multichannel bipolar ablation technique delivers multichannel of RF voltages to the active electrodes. Fig. 1B illustrated the multichannel bipolar ablation mode. In this ablation mode, active electrode 'a' and 'c' are set at $V(t) = A\sin\omega t$, and active electrode 'b' and 'd' are set at $V_{zero}(t) = 0$; the dispersive electrode is not connected. So that the horizontal bipolar currents were induced between each active electrode.

We know that the ablation effect is related to the amplitude has nothing to do with frequency. Therefore in the simulation we reduced the frequencies of two RF sources from $f_1 = 500kHz$ to 0.5 Hz for saving simulation time. However, in a real cardiac ablation scenario a RF frequency is desirable in order to avoid cardiac pacing and nerve stimulation that occurs when low frequency signals are applied to heart.
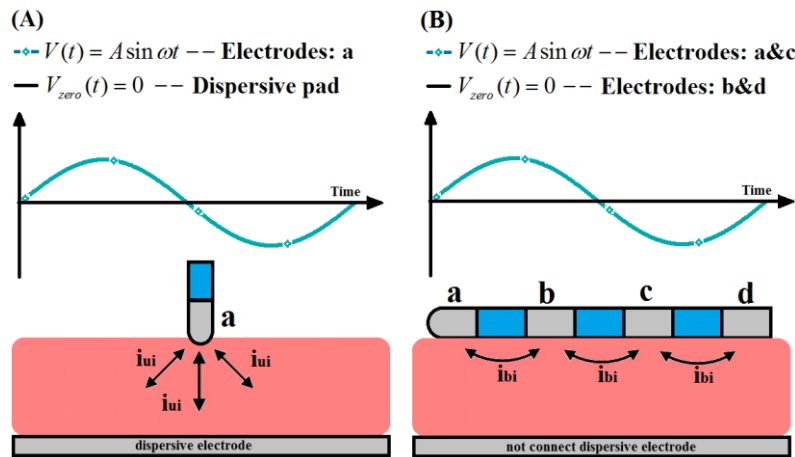
Fig. 1: The principle of unipolar ablation and multichannel bipolar ablation.

2.2. Bio-heat Equation

The physical phenomenon for the coupled thermal-electric problem is governed by the Penne's bio-heat transfer equation [8]:

$$\rho c \frac{\partial T}{\partial t} = \lambda \nabla^2 T + q - Q_b + Q_m \tag{1}$$

Where T, ρ, c, λ, and q are the temperature, density, specific heat, thermal conductivity, and power density, respectively, and Q_b and Q_m represent the blood perfusion and metabolic heat, respectively. The metabolic heat production per volume term Q_m is ignored in our study because it is far smaller than the other

terms [9]. We also ignored the blood tissue and blood perfusion, as was the case in Schutt et al [10]. The power loss produced by the blood flow is modelled by means of forced thermal convection coefficients in the electrodes-blood interface and endocardium-blood interface.

The electrical field problem in the myocardium is solved using the Laplace equation, where σ is the electrical conductivity of myocardium and V is the electric potential.

$$\nabla \cdot (\sigma \nabla V) = 0 \qquad (2)$$

2.3. Construction of the Computer Model

We developed two-dimensional ablation models and used them to represent the two ablation modes. Fig. 2 depicts the two models for cardiac ablation (not to scale). To model UiM ablation, the electrode catheter tip was placed perpendicular to the tissue surface, as shown in Fig. 2A, and to model Multi-BiM, the multipolar catheter, which includes the four active electrodes and three plastic probes, was placed horizontally on the endocardium, as shown in Fig. 2B. A fragment of the connective tissue and the atrial wall was considered in the model [11]. Because the atrial wall thickness ranges from 1.2 to 6.5 mm [12], we constructed an atrial wall of thickness 5 mm.

Model dimensions Z and R were calculated through a convergence analysis to avoid boundary effects, and also the adequate spatial and temporal resolution was estimated using similar convergence test. The maximal temperature (T_{max}) in the tissue after 60 s of ablation was used as the control parameter in the convergence tests. First, a tentative spatial and temporal resolution was considered to determine the appropriate Z and R. We then equally increased Z and R. When the difference in the T_{max} between consecutive simulations was less than 0.5%, we considered the dimensions obtained in the preceding step to be adequate. The dimensions were determined separately for each ablation mode and applied voltage. Finally, by using convergence tests and the same control parameter, we determined the adequate spatial and temporal resolution. The determined values were as follows: Z = R = 90 mm, grid size = 0.5 mm, and time step = 0.05 s for unipolar mode; Z = R = 60 mm, grid size = 0.3 mm, and time step = 0.05 s for multichannel bipolar ablation mode.

In this paper, we used ANSYS 14.0 for building the finite element model and for conducting a solution and Tecplot 360 EX 2015 for post-processing.
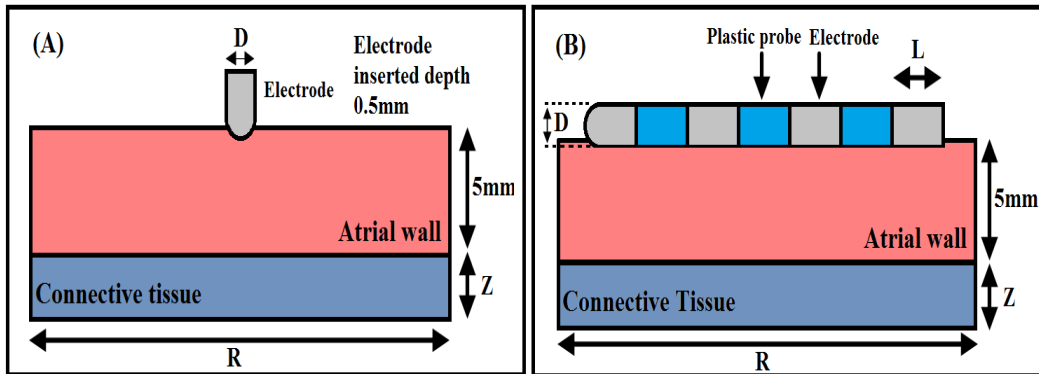
Fig. 2: The geometry of computational model (not to scale). The thickness of atrial wall is 5mm. Details of the electrodes are: Electrode diameter D=2.31mm (7 Fr), electrode lengths L= 4mm, insertion depth 0.5mm and electrode spacing 4mm.

2.4. Material Characteristics

Table I lists the characteristics of the materials considered in the numerical model [11], [13]. The electrical and thermal conductivity of the myocardium was modelled using the temperature-dependent piecewise function [14]. As the temperature increased to less than $100°C$, the electrical conductivity first increased exponentially ($1.5\%/°C$) and then decreased by a factor of 10,000 between $100°C$ and $105°C$ whereas the thermal conductivity increased linearly by $1.2\%/°C$ up to $100°C$, following which it remained constant at temperatures exceeding $110°C$.

Table1: Thermal and electrical characteristics of the elements of the numerical models

Element/material	σ (s/m)	λ (W/m·T)	ρ (kg/m³)	c (J/kg·T)
Electrode	4.6×10^6	71	21500	132
Atrial tissue	0.54	0.53	1060	3111
Plastic Probe	10^{-5}	0.026	70	1045
Connective tissue	0.09	0.4	1000	3200

Measurement temperature at 37°C

2.5. Boundary Condition

Fig. 3 illustrates the electrical boundary conditions of ablation modes. In UiM ablation (Fig. 3A), a constant zero voltage at the border (mimicking the electrical performance of the dispersive electrode), and the active electrode was set at $V(t)=A\sin\omega t$. Fig.3 B shows the ablation mode of four electrodes activated method for creating long continuous lesion in Multi-BiM, where the active electrodes 'a' and 'c' were set at $V(t)=A\sin\omega t$ and the other active electrodes 'b' and 'd' were set at zero voltage to ensure that the electrical currents were forced to flow between each active electrodes. Fig. 3 C-D illustrates the electrical boundary conditions for creating point and short continuous lesion in Multi-BiM. In Fig. 3C the RF source $V(t)=A\sin\omega t$ was applied to the electrode 'a' and zero voltage was applied to the electrode 'b' for creating point lesion. In Fig. 3D the active electrodes 'a' and 'c' were set at $V(t)=A\sin\omega t$, and the electrode 'b' was set at zero voltage for creating short continuous lesion.

The thermal boundary condition was a constant temperature of $T=37°C$ at the border of all models. The cooling effect produced by blood flow inside the atrium was modelled using two forced thermal convection coefficients—708 and 3636 W/m2K—for the endocardium–blood (h_b) and electrode–blood (h_e) interfaces, respectively [15].
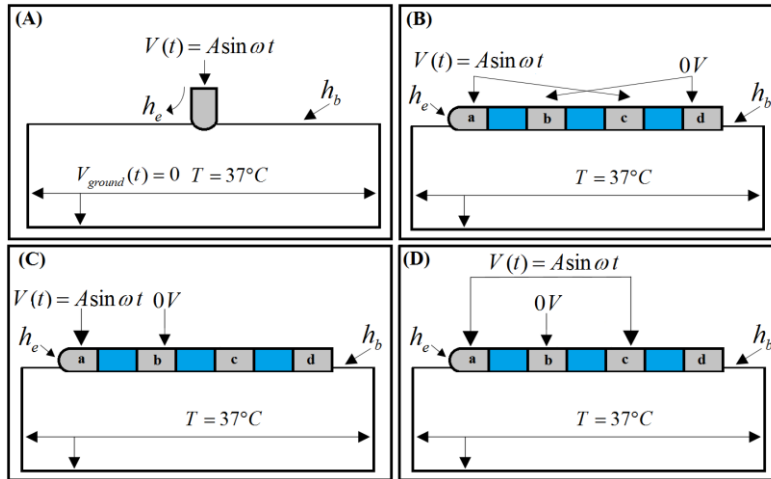
Fig. 3: Electrical and thermal boundary conditions of ablation modes for UiM and Multi-BiM.

3. Results

3.1. Comparison of Unipolar and Multichannel Bipolar Ablation Mode

In our simulation, we compared the ablation effect of UiM-30V and Multi-BiM corresponding to the boundary conditions in Fig. 3A-B. Although tissue injury is the result of several complex mechanisms, thermal lesions created in the atrial wall can be reasonably approximated using an isotherm of 50°C [16]. Fig. 4 presents the temperature distributions and the shapes of the lesion in the atrial wall for the two ablation modes at 60 s. The thermal injury was approximated using the thermal damage borderline: the isotherm of 50°C, which outlines the width and depth of the lesions. Table II lists the maximum depth and width of the lesions created in these ablation modes.

In the UiM-30V ablation, 30V peak value of RF voltage was applied to the active electrode. Because of the low RF voltage (30 V peak value) applied to the active electrode and the blood cooling effect modelled using the forced thermal convection coefficients, UiM-30V ablation failed to create an effective thermal lesion in the atrial wall, and the maximum temperature in the tissue was only 40.09°C (Fig. 4A). In the Multi-BiM ablation, the amplitude of the RF source was adjusted from 20 V to 30 V in 5V steps. In Multi-BiM-20V ablation yielded three discrete lesions between each active electrode (Fig. 4B). As we increased the ablation voltage to 25 V, the Multi-BiM-25V ablation yielded the continuous and symmetrical lesion area: the maximum lesion depth and width were 4.75 mm and 21.25 mm, respectively (Fig. 4C). In Multi-BiM-30V ablation (Fig. 4D), the continuous and transmural lesion was generated in the 5-mm-thick atrial wall. Multi-BiM-30V ablation yielded the symmetrical lesion area: the maximum lesion depth and width were 6.70 mm and 23.50 mm, respectively.

Table2: Lesion dimensions for ablation modes: UiM-30V, Multi-BiM-20V, Multi-BiM-25V and Multi-BiM-30V.

Ablation Modes	Max Depth(mm)	Transmural Depth >5mm	Max Width(mm)	Continuous lesion	Max Tissue temp(°C)
UiM-30V	No	No	No	No	40.09
Multi-BiM-20V	3.36	No	4.23	No	55.70
Multi-BiM-25V	4.75	No	21.25	Yes	63.95
Multi-BiM-30V	6.70	Yes	23.50	Yes	77.32
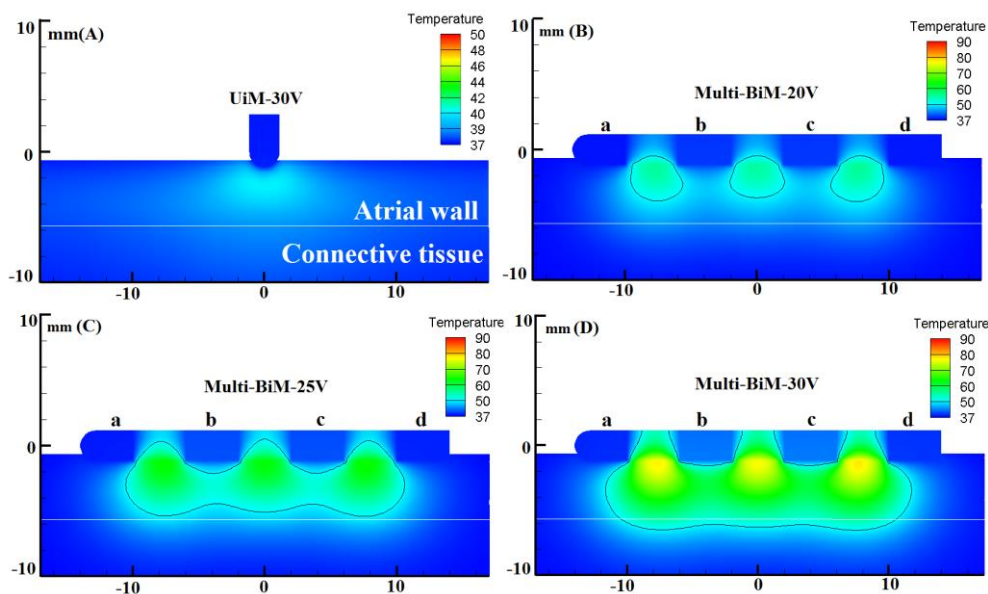
Fig. 4: Temperature distribution in the atrial tissue after 60s of RF ablation across 5mm wall thickness, considering four modes of ablation: (A) UiM-30V, (B) Multi-BiM-20V, (C) Multi-BiM-25V and (D) Multi-BiM-30V. The solid black line is the thermal damage border.

3.2. Multichannel Bipolar Ablation Mode for Creating Discrete and Short Continuous Lesion.

In our simulation, we studied ablation methods of creating discrete and short continuous lesion in multichannel bipolar ablation at 60 s with 30 V peak value voltages corresponding to the boundary conditions in Fig. 3C-D (Multi-BiM-discrete and Multi-BiM-short). Table III lists the maximum depth and width of the lesion created in these ablation modes.

In Multi-BiM-discrete ablation (Fig. 5A), a single transmural lesion was generated in the 5-mm-thick atrial wall with the maximum lesion depth and width were 5.87 mm and 7.89 mm, respectively. In Multi-BiM-short ablation (Fig. 5B), the short continuous and transmural lesion was also generated in the 5-mm-thick atrial wall. Multi-BiM-short ablation yielded the symmetrical lesion area: the maximum lesion depth and width were 5.83 mm and 14.96 mm, respectively.

Table3: Lesion dimensions for ablation modes: Multi-BiM-discrete and Multi-BiM-shotr.

Ablation Modes	Max Depth(mm)	Transmural Depth >5mm	Max Width(mm)	Max Tissue temp(°C)
Multi-BiM-discrete	5.87	Yes	7.89	75.42
Multi-BiM-short	5.83	Yes	14.96	76.21
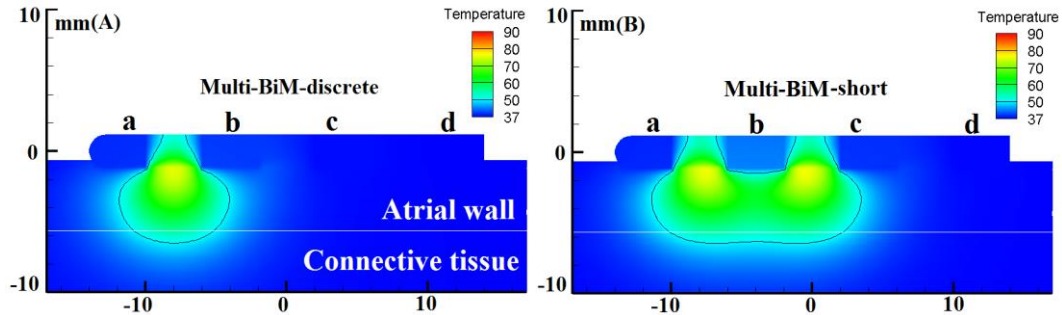
Fig. 5: Temperature distribution in the atrial tissue after 60s of RF ablation across 5mm wall thickness, considering two modes of ablation: (A) Multi-BiM-discrete and (B) Multi-BiM-short. The solid black line is the thermal damage border.

4. Discussion

The main objective of this study was to compare the effectiveness of multichannel bipolar ablation with unipolar ablation in treating AF.

Circumferential ablation around both ipsilateral PVs may be necessary for successfully treating paroxysmal AF and a cornerstone for the ablation of persistent AF supplemented by strategies for further substrate modification, such as creating linear lesions and atrial defragmentation [3]. The results of our computer modelling demonstrate that compared with unipolar ablation, multichannel bipolar ablation can more easily create continuous and large lesion size at low ablation voltage in atrial tissue (seeing Fig.4). In the clinic research, Shin et al. assessed the safety and effectiveness of a novel irrigated multipolar catheter (ten electrodes) for PVI. In their study, unipolar energy was delivered simultaneously in the antral region of the PVs from the nMARQ catheter (Biosense Webster Inc., Diamond Bar, CA, USA) to create ten discrete lesion points [17]. This multichannel RF ablation technique is superior to and is faster than the single ablation technique for PVI, but the orientation of circular catheter must be changed for complete PVI. By contrast, circumferential lesions can be created easily around PVs with minimal or no catheter movement if multichannel bipolar ablation method is applied to the multipolar catheter. Moreover, an additional discrete ablation is also needed for blocking recovery of accessory conduction pathways that caused relapse of AF. Therefore, in our paper we studied the special electrodes activated methods for creating discrete and short continuous lesion in multichannel bipolar ablation. Our results suggest that we can perform an additional discrete ablation or control the length of continuous lesion for PVI and LA ablation through activating special electrodes, such as creating discrete or short continuous lesion (seeing Fig. 5)

In our computer modelling the greater thermal extent are created in multichannel bipolar ablation mode compared with unipolar ablation mode because the higher ablation voltage is induced between adjacent electrodes and it is know that the bipolar voltage contributes to the formation of continuous and deeper lesions. These findings are consistent with those of Gizurarson et al., who studied bipolar energy to create linear and deeper lesions in an in vivo experiment [18]. Some theoretical studies have concluded that unipolar ablation can create discrete lesions and transmural lesions on 1–3 mm thick myocardium but at high ablation voltage and power, for example, at 42.5 V amplitude and 35 W [11], [19]. Whereas the multichannel bipolar ablation technology can create transmural lesions in 5-mm-thick atrial walls with low ablation voltage (30 V peak value).

In cardiac ablation procedure, the esophageal fistula and PV stenosis may occur due to the undesirable extension of the thermal damage depth [20]. We discover that the occurrence of maximal temperature point is beneath the plastic catheter in Multi-BiM ablation, whereas, in unipolar ablation the maximal temperature point is near to the active electrode [21]. We know that that the temperature sensor is usually attached to the metallic electrode to sense real-time temperature, therefore the target temperature should be set lower in order to avoid the excessive thermal damage appeared between the active electrodes when using the Multi-BiM ablation.

5. Limitation

This study has certain limitations. We used a non-irrigated catheter to perform cardiac ablation. To create complete transmural lesions or deeper lesions in the thick atria, irrigated catheter should be used [22].

The blood flow was modelled using a fixed convection coefficient on the electrode–blood and endocardium–blood interface, which is only representative of a constant blood flow rate. But in clinic applications, the blood flow rate varies with the heart diastolic and systolic variables [23]. An accurate method to model the blood flow was consider the blood as a laminar fluid flow with the high and low flow velocities instead of using convective boundary conditions [24], [25]. Therefore, temperature distribution in tissue region varies slightly because of the varying blood flow rate in one cardiac cycle. Moreover, the blood tissue and blood perfusion are ignored in simulations. In simulation models, we have determined the ablation voltage amplitude and ablation time to restrict the maximum tissue temperature less than 100°C during the entire procedure. Therefore, we have not considered the phase change in tissue vaporization to simulate its dissection when it reaches a temperature higher than 100ºC.

6. Conclusion

The simulation results demonstrate that, compared with unipolar ablation, multichannel bipolar ablation can more easily create transmural lesions, continuous lesions and larger discrete lesion size at low ablation voltage in atrial tissue for completing circumferential PVI and LA linear ablation. To validate the theoretical results in this study, an in vitro experiment will be performed in the future works.

7. Acknowledgements

8. References

[1] C. D. Furberget al., "Prevalence of atrial fibrillation in elderly subjects (the Cardiovascular Health Study)," *Am J Cardiol,* 199474(3):236-41.

[2] Y. Wanget al., "Evaluation of Linear Lesions in the Left and Right Atrium in Ablation of Longstanding Atrial Fibrillation," *Pacing and Clinical Electrophysiology,* 2013, 36:1202-1210.

[3] M. D. O'Neillet al., "Long-term follow-up of persistent atrial fibrillation ablation using termination as a procedural endpoint," *Eur Heart J,* 2009, 30(9):1105-1112.

[4] J. M. Guerraet al., "Effects of Open-Irrigated Radiofrequency Ablation Catheter Design on Lesion Formation and Complications:In Vitro Comparison of 6 Different Devices," *J Cardiovasc Electr,* 2013, 24:1157-1162.

[5] S. Spitzeret al., "Multielectrode phased radiofrequency ablation compared with point by point ablation for pulmonary vein isolation outcomes in 539 patients," *Research Reports in Clinical Cardiology,* 2014, 5:11-20.

[6] S. Basuet al., "How effective is bipolar radiofrequency ablation for atrial fibrillation during concomitant cardiac surgery?" *Interact Cardiov Th,* 2012, 15(4): 741-748.

[7] F. Rodriguez Entemet al., "Initial experience and treatment of atrial fibrillation using a novel irrigated multielectrode catheter: Results from a prospective two-center study," *Journal of Arrhythmia,* 2016, 32(2):95-101.

[8] H. H. Penns, "Analysis of tissue and arterial blood temperatures in the resting human forearm," *Journal of applied physiology,* 1948, 1(2): 93-122.

[9] R. M. Irastorzaet al., "Computer modelling of RF ablation in cortical osteoid osteoma: Assessment of the insulating effect of the reactive zone," *Int J Hyperthermia,* 2016, 32(3):221-30.

[10] D. Schuttet al., "Effect of electrode thermal conductivity in cardiac radiofrequency catheter ablation: a computational modeling study," *Int J Hyperthermia,* 2009, 25:99-107.

[11] J. J. Perezet al., "Electrical and Thermal Effects of Esophageal Temperature Probes on Radiofrequency Catheter Ablation of Atrial Fibrillation: Results from a Computational Modeling Study," *J Cardiovasc Electr,* 2015, 26(5):556-564.

[12] S. Y. Hoet al., "Anatomy of the left atrium: Implications for radiofrequency ablation of atrial fibrillation," *J Cardiovasc Electr,* 1999, 10(11):1525-1533.

[13] A. Gonzalez-Suarezet al., "Radiofrequency cardiac ablation with catheters placed on opposing sides of the ventricular wall: Computer modelling comparing bipolar and unipolar modes," *Int J Hyperthermia,* 2014, vol. 30(6):372-384.

[14] M. Trujillo and E. Berjano, "Review of the mathematical functions used to model the temperature dependence of electrical and thermal conductivities of biological tissue in radiofrequency ablation," *Int J Hyperthermia,* 2013, 29(6):590-597.

[15] D. Schuttet al., "Effect of electrode thermal conductivity in cardiac radiofrequency catheter ablation: A computational modeling study," *Int J Hyperther,* 2009, 25:99-107.

[16] D. Shinet al., "Initial results of using a novel irrigated multielectrode mapping and ablation catheter for pulmonary vein isolation," *Heart Rhythm,* 2014, 11(3):375-383.

[17] S. Gizurarsonet al., "Bipolar ablation for deep intra-myocardial circuits: human ex vivo development and in vivo experience," *Europace,* 2014, 16(11):1684-1688.

[18] E. J. Berjano and F. Hornero, "Thermal-Electrical Modeling for Epicardial Atrial Radiofrequency Ablation," *Ieee T Bio-Med Eng,* 2004, 51(8):1348-1357.

[19] J. G. Ravenel and H. P. McAdams, "Pulmonary venous infarction after radiofrequency ablation for atrial fibrillation," *Am J Roentgenology,* 2002, 178(3): 664-666.

[20] A. G. Suarezet al., "Mathematical modeling of epicardial RF ablation of atrial tissue with overlying epicardial fat," *Open Biomed Eng J,* 2010, vol. 4: 47-55.

[21] J. Gopalakrishnan, "A Mathematical Model for Irrigated Epicardial Radiofrequency Ablation," *Ann Biomed Eng,* 2002, 30(7):884 - 893.

[22] S. Tungjitkusolmunet al., "Guidelines for predicting lesion size at common endocardial locations during radio-frequency ablation," *Ieee T Bio-Med Eng,* 2001, 48(2): 194-201.

[23] A. Gonzalez-Suarez and E. Berjano, "Comparative Analysis of Different Methods of Modeling the Thermal Effect of Circulating Blood Flow During RF Cardiac Ablation," *IEEE T Bio-Med Eng,* 2016, 63(9): 250-259.

[24] M. K. W. Jain, "A Three-Dimensional Finite Element Model of Radiofrequency Ablation with Blood Flow and its Experimental Validation," *Ann Biomed Eng,* 2000, 28(9): 1075 - 1084.